All-Electron First Principles Calculations of the Ground and Some Low-Lying Excited States of BaI

Evangelos Miliordos, Aristotle Papakondylis, Athanasios A. Tsekouras, and Aristides Mavridis*

Laboratory of Physical Chemistry, Department of Chemistry, National and Kapodistrian University of Athens, P.O. Box 64 004, 157 10 Zografou, Athens, Greece

Received: June 13, 2007; In Final Form: July 18, 2007

The electronic structure of the heavy diatomic molecule BaI has been examined for the first time by *ab initio* multiconfigurational configuration interaction (MRCI) and coupled cluster (RCCSD(T)) methods. The effects of special relativity have been taken into account through the second-order Douglas−Kroll−Hess approximation. The construction of $\Omega(\omega,\omega)$ potential energy curves allows for the estimation of "experimental" dissociation energies (D_e) of the first few excited states by exploiting the accurately known D_e experimental value of the $X^2\Sigma^+$ ground state. All states examined are of ionic character with a Mulliken charge transfer of 0.5 e^- from Ba to I, and this is reflected to large dipole moments ranging from 6 to 11 D. Despite the inherent difficulties of a heavy system like BaI, our results are encouraging. With the exception of bond distances that on the average are calculated 0.05 Å longer than the experimental ones, common spectroscopic parameters are in fair agreement with experiment, whereas D_e values are on the average 10 kcal/mol smaller.

1. Introduction

The barium iodide radical, BaI, was first identified as early as 1870 in an absorption spectrum by de Boisbaudran who recorded two bands at 537.6 and 560.7 nm, along with analogous bands for BaCl and BaBr.[1] In 1906 the results of de Boisbaudran were corroborated by Olmsted, who recorded two broad bands at ∼537 and ∼561 nm, which were attributed to BaI by analogy with the spectra of other alkaline-earth monohalides.[2] These observations were confirmed in 1928 by Walters and Barratt[3] who reproduced the same bands noticing also some absorption in the region of 380 nm. In 1939, Mesnage[4] determined the heads of the two Olmsted bands at 538.3 and 561.2 nm. These absorptions, which correspond to the $C^2\Pi_{3/2}-X^2\Sigma^+$ and $C^2\Pi_{1/2}-X^2\Sigma^+$ subbands of the $C^2\Pi-X^2\Sigma^+$ transition, were again analyzed by Patel and Shah in 1970, who also reported that the ∼380 nm absorption was due to the $E^2\Sigma^+-X^2\Sigma^+$ and $D^2\Sigma^+-X^2\Sigma^+$ transitions.[5] In 1974, Zare and co-workers measured radiative lifetimes of the $C^2\Pi_{1/2}$ and $C^2\Pi_{3/2}$ states.[6] One year later, Bradford et al.[7] studied the chemiluminescence produced when BaI was formed in the gas-phase reaction of Ba with I_2. The emission recorded in the infrared region was recognized to be the result of the $A^2\Pi-X^2\Sigma^+$ and $B^2\Sigma^+-X^2\Sigma^+$ electronic transitions. From the chemiluminescence spectrum of the Ba + I_2 reaction, Zare and co-workers[8] suggested a lower bound for the BaI dissociation energy, $D_0 \geq 102 \pm 1$ kcal/mol (retracted in a later publication and attributed to experimental complications; see ref 11). A comprehensive study of the $C^2\Pi-X^2\Sigma^+$ bandheads followed by Shah and Patel,[9] showed that both subbands of the spectrum consist mainly of the $\Delta v = 0$ sequence with Franck−Condon factors close to unity. In the same year Rao et al.,[10] studied the visible emission spectra of BaI providing vibrational constants for the $C^2\Pi$ and $X^2\Sigma^+$ states. A new value for $D_0 = 72.9 \pm 2$ kcal/mol was proposed one year later by Estler and Zare by using time-of-flight single-collision chemiluminescence spectroscopy.[11] This value is in harmony with $D_0 = 71.4 \pm 1.0$ kcal/mol obtained in the same year by high-temperature mass spectrometry.[12] During the 1980s and early 1990s a significant amount of work on BaI was published, mainly by the group of Zare, focused on the rotational structure of BaI.[13−20]

For the first time the electric dipole moment of the $X^2\Sigma^+$ state of BaI was determined in 1986 by high-precision Stark spectroscopy, $\mu = 5.969$ D,[21] indicative of ionic bonding. In a paper published in 1990 by Fernando et al.[22] on BaOH, a new state of BaI was observed tagged $A'^2\Delta$, implying that this is the first excited state of BaI,[23] as indeed was confirmed later (see ref 28). The same year Zare and co-workers,[24] through application of energy-balance arguments to the crossed-beam reaction Ba + HI → BaI + H, provided a new value of the lower limit for the dissociation energy of BaI, $D_0 \geq 76.8 \pm 1.7$ kcal/mol, recommending finally $D_0 = 77.7 \pm 2.0$ kcal/mol. Two years later Hildenbrand and Lau[25] corrected their previously reported value[12] of $D_0 = 71.4 \pm 1.0$ to $D_0 = 76.2 \pm 1.5$ kcal/mol, in agreement with the final result of ref 24. In the years 1999−2001 Gutteres et al. published a sequence of four papers where they present an extensive study of six low-lying electronic states of the BaI molecule.[26−29] These workers used the Fourier transform laser-induced fluorescence spectroscopy method to obtain very accurate spectroscopic parameters of the $X^2\Sigma^+$, $A'^2\Delta_{3/2}$, $A^2\Pi$, $B^2\Sigma^+$, $C^2\Pi$, and $D^2\Sigma^+$ states of BaI.

It is clear by now that BaI from the beginning of its identification has attracted the attention of the experimentalists. It is remarkable, however, notwithstanding the inherent difficulties of a heavy system, that no ab initio or even density functional theory calculations exist in the literature on BaI. To the best of our knowledge, only semiempirical approaches such as the electrostatic polarization model,[30,31] ligand field theory,[32] and the quantum defect theory[33,34] were employed to predict properties of the ground and excited states. Barium monoiodide is the heaviest nonradioactive member of the alkaline-earth monohalides family. The size of the system, 109 electrons and two very heavy nuclei of $Z = 56$ (Ba) and 53 (I), introduces

* Corresponding author. E-mail address: mavridis@chem.uoa.gr.

10.1021/jp0745788 CCC: $37.00
Published on Web 09/13/2007

intractable correlation and relativistic problems for accurate all-electron ab initio calculations; the absence of high-quality basis sets is an additional source of difficulty.

This is the first effort for obtaining all-electron ab initio results using conventional methods; the purpose is two-fold: First, to benchmark our techniques vs the existing accurate experimental results, and second, to better understand the electronic structure of BaI and to supply the experimentalists with some new information, perhaps useful to their future investigations on this not so easily tamable molecule. To this end we have constructed full potential energy curves for the first nine bound states of BaI, namely, $X^2\Sigma^+$, $A'^2\Delta$, $A^2\Pi$, $B^2\Sigma^+$, $C^2\Pi$, $D^2\Sigma^+$, $3^2\Pi$, $4^2\Sigma^+$, and $5^2\Sigma^+$. We report binding energies, dipole moments, usual spectroscopic parameters, and spin−orbit interactions, through multireference and coupled-cluster methods corrected for scalar relativistic effects.

2. Computational Approach

As already mentioned, a problem for the present work is the lack of quality all-electron basis sets. For the purpose of this study a basis set capable of describing adequately some of the excited states of Ba and Ba^+ is needed. We chose to use the well-tempered basis set (WTBS) of Huzinaga et al.,[35] for both the Ba and I atoms. It seems that this is the largest all-electron basis set for Ba existing in the literature, but optimized only for its ground state (^{1}S).

For Ba, the uncontracted (30s23p17d) basis augmented by a d and two f functions ($\zeta_d = 0.09$, $\zeta_{1f} = 0.85$, $\zeta_{2f} = 0.40$) and generally contracted to [9s7p5d2f] was used. The ζ_d, ζ_{1f}, and ζ_{2f} values were determined by optimizing the Ba ^{3}D−^{1}S gap at the CISD valence ($6s^2$) level with respect to the experimental energy separation. The primitive iodine basis was also augmented by two f functions with exponents $\zeta_1 = 2.5$, $\zeta_2 = 0.45$ (28s23p17d2f) obtained by optimizing the total energy of the iodine ^{2}P state (CISD), and similarly contracted to [8s7p5d2f]. The complete one-electron space contains a total of 137 spherical Gaussians.

Potential energy curves (PEC) were obtained through the complete active space self-consistent field (CASSCF)+single+double replacements (CASSCF+1+2 ≡ MRCI) method. The restricted coupled-cluster+singles+doubles+perturbative connected triples [RCCSD(T)][36] method was also employed, limited of course around equilibrium geometries and for those states accessible by a single reference method.

The reference (CASSCF) wave functions were constructed by allotting the seven "valence" electrons ($6s^2_{Ba} + 5p^5_I$) to 12 valence orbitals (one s + three p + five d on Ba and three p on I). The two valence 5s electrons of the I atom were excluded from the active space for purely technical reasons, but of course they were included at the MRCI level. Our CAS wavefunctions comprise about 14000 configuration functions (CF), giving rise in turn to MRCI expansions varying form (20−25) × 10^6 CFs. These expansions were further reduced by an order of magnitude by applying the internal contraction technique[37] as implemented in the MOLPRO package.[38] MRCI and RCCSD(T) calculations were also performed including the $5s^25p^6$ "core" electrons of the Ba atom (C-MRCI/C-RCCSD(T)). To make these C-MRCI feasible, a threshold of 0.001 was applied to the CASSCF wavefunctions, i.e., CFs with coefficients smaller than 0.001 were discarded, reducing the C-MRCI spaces to about 44 × 10^6 CFs.

Using the state average approach, spin−orbit (SO) splittings for the Π and Δ states were obtained by diagonalizing the Breit−Pauli Hamiltonian within the space of all studied states at the MRCI and C-MRCI level.[38]

Spectroscopic constants for all states are extracted by solving numerically the one-dimensional rovibrational Schrödinger equation. Scalar relativistic effects were taken into account through the second-order Douglas−Kroll−Hess approximation (DKH2),[39] recontracting the same basis set at the CASSCF+DKH2 (for Ba) and spherically averaged SCF+DKH2 (for I) level. The basis set superposition error (BSSE)[40] of the $X^2\Sigma^+$ state was estimated with respect to $Ba^+(^2S)$ and $I^-(^1S)$ at the C-MRCI(+Q) and C-RCCSD(T) level, and it is found to be 2.02 (2.48) and 2.69 kcal/mol, respectively. Dissociation energies were obtained through the supermolecule approach at 20 bohr.

All calculations were performed with the MOLPRO2002.6 suite of codes.[38]

3. Chemical Insights

The ground states of Ba and I atoms are $^1S(6s^2)$ and $^2P(5s^25p^5)$, respectively. They give rise to a $^2\Sigma^+$ and a $^2\Pi$ state, apparently of repulsive nature, but interacting severely through avoided crossings with ionic bound states of $^2\Sigma^+$ and $^2\Pi$ symmetry (vide infra). The first excited state of Ba is $^3D(6s^15d^1)$, 9357 cm^{-1} (M_J averaged) above its ground state, whereas the first excited state of I is $^4P(5s^25p^46s^1)$ located 58073 cm^{-1} higher than the ^{2}P state.[41] From $Ba(^3D) + I(^2P)$ one obtains a total of 18 $^{2S+1}|\Lambda|$ states, namely Φ[1], Δ[2], Π[3], Σ^+[2], Σ^-[1] doublets and quartets. Obviously, the quartets should be repulsive, and indeed they are. From the doublets, one Σ^+ state, the Σ^- two of the Π states, one Δ and one Φ state are also of repulsive character according to our calculations. This can also be seen from the following valence-bond-Lewis (vbL) diagram.

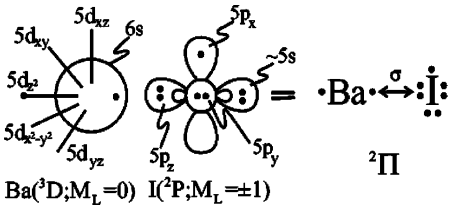

The above $^2\Pi$ state is clearly repulsive. Moving the $5d_{z^2}$ ($M_L = 0$) electron to the $5d_\pi$ ($5d_{xz}$ or $5d_{yz}$) Ba atomic orbitals ($M_L = \pm 1$), the $^2\Sigma^+$, $^2\Sigma^-$ and $^2\Delta$ states are obtained. In principle, all three could be attractive but the σ-repulsion seems to prevail. Finally, moving the Ba d-electron to the $5d_\delta$ ($5d_{xy}$ or $5d_{x^2-y^2}$) orbitals ($M_L = \pm 2$) forms the BaI $^2\Pi$ and $^2\Phi$ states, which do not have any reason to be attractive.

The remaining three doublets, i.e.,$^2\Sigma^+$, $^2\Pi$, $^2\Delta$ with the in situ I in the $M_L = 0$ ($5p^1_z$) component could be of attractive nature, but their interaction with states of the same symmetry of Coulombic origin (see below) obscures their character.

The experimental ionization energy (IE) of Ba is 5.21 eV,[41] and the electron affinity (EA) of I is 3.37 (M_J averaged) eV.[42] Certainly the small energy difference IE − EA = 1.84 eV suggests an ionic molecule Ba^+I^-; therefore we can comprehend much better the molecular states of BaI as resulting from the ground and excited states of Ba^+ in the field of the closed shell $I^-(^1S)$ anion. Naturally, this approach leads to doublets only, their symmetries being determined by the symmetry of the Ba^+ cation:

$$Ba^+(^2S;\, 6s^1) + I^-(^1S) \rightarrow X^2\Sigma^+ \quad (1)$$

$$Ba^+(^2D;\, 5d^1) + I^-(^1S) \rightarrow A'^2\Delta,\ A^2\Pi,\ B^2\Sigma^+ \quad (2)$$

$$Ba^+(^2P;\,6p^1) + I^-(^1S) \rightarrow C^2\Pi,\, 4^2\Sigma^+ \quad (3)$$

$$Ba^+(^2S;\,7s^1) + I^-(^1S) \rightarrow D^2\Sigma^+ \quad (4)$$

With the exception of the $4^2\Sigma^+$ state, we follow the spectroscopic notation of the experimentalists tagging as A′ the first excited state of $^2\Delta$ symmetry.[22,28] Notice that the $D^2\Sigma^+$ state correlates to a Rydberg $Ba^+(^2S;\,7s^1)$ atomic state. The experimental energy separations of Ba^+ (M_J averaged), namely $^2D \leftarrow {}^2S$, $^2P \leftarrow {}^2S$, and $^2S(7s^1) \leftarrow {}^2S(6s^1)$ are 5354, 21389, and 42355 cm^{-1}, respectively.[41]

4. Results and Discussion

Table 1 lists the energetics of Ba and I atoms and their ions calculated at various levels of theory. With the exception of the energy separations $Ba(^3D \leftarrow {}^1S)$ and $Ba^+(^2D \leftarrow {}^2S)$, where there are significant discrepancies from the corresponding experimental numbers, the rest of the values are in relatively good agreement with experiment. The admittedly large differences between theory and experiment are observed when relativistic effects were taken into account. We surmise that this is due to the basis set not tuned for this kind of calculations.

Table 2 shows total energies, dissociation energies (D_e), common spectroscopic parameters and dipole moments (μ) of the states $X^2\Sigma^+$, $A'^2\Delta$, $A^2\Pi$, $B^2\Sigma^+$, $C^2\Pi$, and $D^2\Sigma^+$ along with available experimental values; Figures 1 ($\Lambda-\Sigma$) and 2 (Ω) display potential energy curves at the (valence) MRCI level of theory. We discuss first the ground state, then the states $A'^2\Delta$, $A^2\Pi$, $B^2\Sigma^+$ of channel (2), followed by the rest of the states.

$X^2\Sigma^+$. The ground state of BaI correlates adiabatically to $Ba(^1S) + I(^2P;M_L=0)$, acquiring ionic character after an avoided crossing at about 7.5 Å, with the ionic end products $Ba^+(^2S) + I^-(^1S)$ (experimentally) 1.84 eV (M_J averaged) above the neutral ones; Figure 1. As expected a single configuration describes adequately this state, namely $|X^2\Sigma^+\rangle = 0.97|(\text{core})^{102}\ 1\sigma^2 2\sigma^1 1\pi_x^2 1\pi_y^2\rangle$ at the CASSCF level and counting the seven "valence" $[6s^2(Ba)+5p^5(I)]$ electrons only. According to the Mulliken population analysis more than $0.5e^-$ is transferred from Ba to I. Obviously, the molecule should acquire its ionic character after the avoided crossing, $(IE - EA)/27.2114 = 1/r$, or $r = 14.8$ bohr (=7.8 Å), whereas at the equilibrium $\sim 0.3e^-$ and $\sim 0.2e^-$ are transferred from I^- to Ba^+ through the σ and π paths, respectively.

At the MRCI level, $r_e = 3.251$ Å, 0.16 Å larger than the experimental one;[26,27,29] Table 1. By including the $5s^25p^6$ electrons of Ba (C-MRCI), the bond distance decreases by about 0.12 Å, a dramatic improvement. The same is observed at the RCCSD(T) vs C-RCCSD(T) level, whereas the role of scalar relativistic effects seems to be of minor importance. At the highest level of theory C-MRCI+DKH2+Q (C-RCCSD(T)+DKH2) $r_e = 3.140$ (3.136) Å, still 0.05 Å longer than the experimental value. Including first the $4d^{10}$ electrons of I and subsequently the $4d^{10}$ electrons of both atoms in the C-RCCSD(T) calculation, the bond distance becomes 3.130 Å ($\delta r_1 \equiv 3.137 - 3.130 = 0.007$ Å), and finally 3.121 Å ($\delta r_2 \equiv 3.130 - 3.121 = 0.009$ Å), respectively. The bond distance remains practically unchanged by further including in the C-RCCSD(T) calculations the $4s^24p^6$ electrons of Ba. Recalculating now the bond distance at the C-RCCSD(T) level but taking into account the BSSE correction, the r_e increases to 3.149 Å as compared to the uncorrected one 3.137 Å by $\delta r_3 \equiv 3.149 - 3.137 = 0.012$ Å. Assuming additivity of the successive core (δr_1, δr_2) effects and BSSE (δr_3), our final equilibrium distance at the C-RCCSD(T)+DKH2 level becomes $3.136 - \delta r_1 - \delta r_2 + \delta r_3 = 3.136 - 0.007 - 0.009 + 0.012 = 3.132$ Å, a practical cancellation of $\delta r_1 + \delta r_2$ and δr_3 effects. For this reason the δr corrections will be no considered any further.

The analysis of D_e is more involved. The first column of D_e values in Table 1 refers to $\Lambda-\Sigma$ dissociation energies, i.e., with respect to $Ba(^1S) + I(^2P)$, whereas D_e numbers in parentheses refer to dissociation energies with respect to $Ba(^1S_0) + I(^2P_{3/2})$. The SO splitting of I ($^1/_2 \leftarrow {}^3/_2$) is calculated to be 6211 (CISD) and 8052 (CISD+DKH2) cm^{-1}, as compared to the experimental value of 7603.2 cm^{-1} (ref 41). D_e values with and without scalar relativistic effects were corrected by subtracting the one-third of the CISD+DKH2 and CISD SO splittings, i.e., 2070 and 2685 cm^{-1}, respectively. Although the scalar relativistic effects do not seem to influence the D_e value at the C-MRCI level (74.2 vs 75.1 kcal/mol), adding the Davidson correction we obtain (C-MRCI+DKH2+Q) $D_e = 68.3$ kcal/mol. The same value is obtained practically at the CCSD(T)+DKH2 or C-RCCSD(T)+DKH2 level of theory. Considering the latter value and subtracting the BSSE effect we get D_e(C-RCCSD(T)+DKH2-BSSE) = 69.3 − 2.69 = 66.6 kcal/mol. The corresponding value at the multireference level is D_e(C-MRCI+DKH2+Q-BSSE) = 68.3 − 2.48 = 65.8 kcal/mol. Ignoring the zero point energy ($\sim\omega_e/2 = 0.2$ kcal/mol), our calculated value $D_e = 66.2$ [$=^1/_2(66.6 + 65.8)$] kcal/mol differs by 10 kcal/mol from the experimental number, an understandable discrepancy considering the vicissitudes of the BaI system. It is interesting, however, that the best D_e values as compared to experiment is obtained at the C-MRCI+Q level (75.2 kcal/mol), due to a happy cancellation of errors.

We can claim that, on the average, the ω_e, $\omega_e x_e$, a_e, and $\bar{D}_e$ spectroscopic parameters are in good agreement with experiment. At the highest level of theory C-MRCI+DKH2+Q (C-RCCSD(T)+DKH2), the dipole moment is slightly overestimated with respect to the experimental value, 6.21 (6.35) vs 5.97 Debye.[21]

$A'^2\Delta$, $A^2\Pi$, and $B^2\Sigma^+$. The $A'^2\Delta$ and $B^2\Sigma^+$ states correlate adiabatically to $Ba(^3D) + I(^2P)$ whereas $A^2\Pi$ to $Ba(^1S) + I(^2P)$, but diabatically all three correlate to $Ba^+(^2D) + I^-(^1S)$ due to avoided crossings with incoming ionic states of the same symmetry (experimentally) 2.50 eV [=IE(Ba) − EA(I) + $\Delta E(Ba^+;{}^2D \leftarrow {}^2S)$] higher than the ground end products. In the field of $I^-(^1S)$ the degeneracy of the $M_L = \pm 2, \pm 1, 0$ components of the Ba^+ ^2D components is lifted, resulting in the $^2\Delta$, $^2\Pi$, and $^2\Sigma^+$ molecular states, respectively. Their energy ordering is expected to be $A'^2\Delta < A^2\Pi < B^2\Sigma^+$ with rather relatively small energy separations: The $5d_{xy}(\delta_-)$ or $5d_{x^2-y^2}(\delta_+)$ electron on Ba^+, which gives rise to the $^2\Delta$ state, interacts less repulsively with the incoming closed shell anion I^- than the $5d_{z^2}(d_\sigma)$ distribution that gives rise to the $^2\Sigma^+$ state. This is indeed the experimental ordering with energy separations of about 1000 cm^{-1}; see Table 2 and Figure 1. Counting only the seven "valence" electrons, the leading CASSCF CFs are $|A'^2\Delta\rangle = 0.98|(\text{core})^{102}\ 1\sigma^2 1\pi_x^2 1\pi_y^2 1\delta^1\rangle$, $|A^2\Pi\rangle = 0.96|(\text{core})^{102}\ 1\sigma^2 1\pi_x^2 1\pi_y^2 2\pi^1\rangle$, and $|B^2\Sigma^+\rangle = 0.97|(\text{core})^{102}\ 1\sigma^2 3\sigma^1 1\pi_x^2 1\pi_y^2\rangle$.

At the "simple" MRCI or MRCI+Q level, the bond lengths of all three states are about 0.20 Å longer than the experimental values. Including the $5s^25p^6$ "core" electrons of Ba (C-MRCI or C-RCCSD(T)) the same pattern is followed as in the $X^2\Sigma^+$ state (i.e., the bond length is reduced by 0.10−0.12 Å), whereas scalar relativistic effects are responsible for a further reduction of 0.03−0.05 Å. At the highest level of theory C-MRCI+DKH2+Q (C-RCCSD(T)+DKH2), the bond distances of $A'^2\Delta$, $A^2\Pi$, and $B^2\Sigma^+$ states become 3.192 (3.188), 3.195 (3.190), and

TABLE 1: Total Energies *E* (hartree) of Ba(^{1}S) and I(^{2}P), Ionization Energies IE (eV) of Ba, Electron Affinities EA (eV) of I, and Energy Gaps (cm^{-1}) of Ba(^{1}D,^{3}D←^{1}S) and Ba$^+$(^{2}P,^{2}D,^{2}S←^{2}S) in Differenet Methods

method[a]	$-E$(Ba)	$-E$(I)	IE(Ba)	EA(I)	Ba[^{3}D($6s^15d^1$)←^{1}S($6s^2$)]	Ba$^+$[^{2}D($5d^1$)←^{2}S($6s^1$)]	Ba$^+$[^{2}P($6p^1$)←^{2}S($6s^1$)]	Ba$^+$[^{2}S($6s^1$)←^{2}S($7s^1$)]
CISD	7883.56692	6918.11192	4.717	2.953	8701	2087[b]	18180[b]	37143[b]
CISD+Q		6918.1210		2.997				
CISD+DKH2	8129.16019	7110.99379	4.905	2.885	13298	7316[b]	20052[b]	38750[b]
CISD+DKH2+Q		7111.0022		2.936				
C-CISD[c]	7883.74623		4.910		7786	1944	18983	39554
C-CISD+Q[c]	7883.7608		4.981		7905	1961	19085	39916
C-CISD+DKH2[c]	8129.33550		5.047		12477	7530	21266	41292
C-CISD+DKH2+Q[c]	8129.3488		5.114		12565	7560	21386	41656
RCCSD(T)		6918.12089		3.027				
RCCSD(T)+DKH2		7111.00222		2.965				
C-RCCSD(T)[c]	7883.76203		4.987		7964	2024	19149	39944
C-RCCSD(T)+DKH2[c]	8129.34500		5.118		12620	7630	21450	
expt			5.210[d]	3.373[e]	9357.027[d,f]	5354.434[d,f]	21388.81[d,f]	42355[d]

[a] +Q refers to the Davidson correction and DKH2 to Douglas−Kroll−Hess second-order relativistic correction. [b] Hartree−Fock calculations. Note that in the case of Ba the (valence) CISD is full-CI. [c] The $5s^25p^6$ "core" electrons of Ba have been included in the CI-procedure. [d] Reference 41. [e] This value has been obtained by adding to the EA of I, EA(I) = E(I;^{2}P$_{3/2}$) − E(I$^-$^{1}S$_0$) = 3.059 eV (ref 42), the weighted average of the SO splitting of I (ref 41): $^1/_3\Delta E_{SO}(^2P_{1/2}-^2P_{3/2}) = {}^1/_3 \times 7603.2$ cm^{-1} = 0.314 eV. [f] M_J averaged values.

3.176 (3.180) Å, respectively, differing by 0.070 (0.066), 0.056 (0.051), and 0.047 (0.051) Å from experiment.

Concerning the energy separations (T_e) from the X$^2\Sigma^+$ state the agreement with experiment cannot be considered as satisfactory. For instance, at the MRCI+DKH2 or MRCI+DKH2+Q level the order of the A$^2\Pi$ and B$^2\Sigma^+$ states is reversed; the same is happening between the A′$^2\Delta$ and A$^2\Pi$ states at the C-MRCI+DKH2 level. Nevertheless, at the highest level of theory C-MRCI+DKH2+Q (C-RCCSD(T)+DKH2) the energy ordering is predicted correctly, namely, T_e = 11281 (11297), 11948 (11954), 12280 (12286) cm^{-1} for (A′$^2\Delta$, A$^2\Pi$, B$^2\Sigma^+$) ← X$^2\Sigma^+$, as contrasted to the experimental values 8369.0 (A′$^2\Delta_{3/2}$),[28,29] 9605.4 (A$^2\Pi$),[27,29] and 10427.0 (B$^2\Sigma^+$).[26,27,29] This large discrepancy of more than 2000 cm^{-1} for all states can be traced to the Ba$^+$(^{2}D←^{2}S) separation calculated as 7560 (7630) cm^{-1} at the same level of theory, higher by 2206 (2276) cm^{-1} from experiment; see Table 1. By parallel shifting the PECs of A′$^2\Delta$, A$^2\Pi$, and B$^2\Sigma^+$ states by 2206 (2276) cm^{-1} (and including the spin−orbit interaction in the A′$^2\Delta_{3/2}$ state equals −615/2 cm^{-1} at the C-MRCI+DKH2 level), the above calculated splittings become T_e = 8767 (8713), 9742 (9678), and 10074 (10010) cm^{-1}, respectively, now in acceptable agreement with experiment.

Because of their complexity we will discuss dissociation energies separately in section 5. Spectroscopic parameters ω_e, $\omega_e x_e$, a_e, and $\bar{D}_e$ are in relatively good agreement with experiment in all methods of calculation (Table 2). In particular, at the C-RCCSD(T)+DKH2 level ω_e values are 135 cm^{-1}, as contrasted to the experimental value of 142 cm^{-1} for all three states A′$^2\Delta$, A$^2\Pi$, and B$^2\Sigma^+$, whereas anharmonic frequencies $\omega_e x_e$ are calculated to be 0.29 (A′$^2\Delta$), 0.26 (A$^2\Pi$), and 0.44 (B$^2\Sigma^+$) cm^{-1} with corresponding experimental values being 0.274, 0.275, and 0.506 cm^{-1}. No experimental dipole moments for the excited states of BaI are available; on the basis of the good agreement between experiment and theory for the X$^2\Sigma^+$ state, we believe that our calculated dipole moments can be considered as reliable enough. We recommend the values μ = 10.5 (A′$^2\Delta$), 8.0 (A$^2\Pi$), and 6.5 (B$^2\Sigma^+$) D. Notice that the dipole moments of the X$^2\Sigma^+$ and B$^2\Sigma^+$ states are very similar, being significantly lower than those of the A′$^2\Delta$ and A$^2\Pi$ states, as expected, due to the polarization of the symmetry defining electron density on the back of the Ba atom in the Σ^+ states.

C$^2\Pi$, D$^2\Sigma^+$, 3$^2\Pi$, 4$^2\Sigma^+$, and 5$^2\Sigma^+$. States C$^2\Pi$, D$^2\Sigma^+$, and 3$^2\Pi$ correlate adiabatically to Ba(^{3}D) + I(^{2}P), but diabatically C$^2\Pi$ correlates to Ba$^+$(^{2}P;$6p^1$) + I$^-$(^{1}S) and D$^2\Sigma^+$ to Ba$^+$(^{2}S;$7s^1$) + I$^-$(^{1}S), whereas the 3$^2\Pi$ state results from an avoided crossing of a repulsive $^2\Pi$ state emanating from Ba(^{1}S)+I(^{2}P) and the C$^2\Pi$ state (see Figure 1). The 4$^2\Sigma^+$ and 5$^2\Sigma^+$ states correlate adiabatically to the second excited state of Ba (^{1}D), experimentally 11395.4 cm^{-1} above its ground state and 2038.4 cm^{-1} above the first excited state of Ba(^{3}D)[41] + I(^{2}P). However, the diabatic asymptotic fragments of 4$^2\Sigma^+$ are Ba$^+$(^{2}P;$6p^1$) + I$^-$(^{1}S); on the other hand 5$^2\Sigma^+$ is "created" due to the avoided crossing of the 4$^2\Sigma^+$ and a repulsive $^2\Sigma^+$ state correlating to Ba(^{1}S) + I(^{2}P) (see Figure 1). It should be mentioned that no experimental results exist for the 3$^2\Pi$, 4$^2\Sigma^+$, and 5$^2\Sigma^+$ states (but see below).

The calculated bond distances in the C$^2\Pi$ and D$^2\Sigma^+$ states follow the same pattern as before. The MRCI values are significantly larger than the experimental ones, but they improve drastically after the inclusion of the $5s^25p^6$ electrons of the Ba atom at the CI level. At the highest level, C-MRCI+DKH2+Q (C-RCCSD(T)+DKH2), r_e = 3.165 (3.170) and 3.017 Å for the C$^2\Pi$ and D$^2\Sigma^+$ states, respectively. The complete agreement of r_e for D$^2\Sigma^+$ with experiment is rather surprising and can be considered as, partly, fortuitous. Concerning the T_e values, we observe that although the scalar relativistic effects improve the agreement with experiment for the D$^2\Sigma^+$ state, they have the opposite effect in the C$^2\Pi$ state. Interestingly, at the MRCI+Q level the agreement between theory and experiment in the C$^2\Pi$ state, 18839 vs 18188.5 cm^{-1}, can be considered as quite good, but they differ by more than 3000 cm^{-1} at the highest level of theory, C-MRCI+DKH2+Q or RCCSD(T)+DKH2. In the D$^2\Sigma^+$ state the C-MRCI+DKH2+Q T_e value is in excellent agreement with the experimental result, and here the relativistic effects play a significant role toward the right direction.

Recommended dipole moments are μ = 11−12 ($C^2\Pi$) and 5.5 D($D^2\Sigma^+$), following the same pattern as before, i.e., the Σ^+ symmetry μ values being considerably lower than the Δ or Π ones.

The rest of the calculated spectroscopic constants, ω_e, $\omega_e x_e$, a_e, and $\bar{D}_e$ are in "logical" agreement with the experimental values; dissociation energies will be discussed in the next section.

The calculation of the 3$^2\Pi$, 4$^2\Sigma^+$, and 5$^2\Sigma^+$ presents insurmountable technical difficulties due to multiple avoided crossings. Within the $\Lambda-\Sigma$ ansatz we have obtained PECs at the MRCI level shown in Figure 1, and a very limited set of numbers of questionable validity (see Table 2). Experimentally, a state assigned as G$^2\Sigma^+$ has been observed at about 30000

TABLE 2: Total Energies E (hartree), Bond Distances r_e (Å), Dissociation Energies D_e (kcal/mol), Harmonic and Anharmonic Frequencies ω_e and $\omega_e x_e$ (cm^{-1}), Rotational−Vibrational Coupling Constants a_e ($\times 10^{-5}$ cm^{-1}), Centrifugal Distortions $\bar{D}_e$ ($\times 10^{-9}$ cm^{-1}), Dipole Moments μ(D), and Energy Separations from the Ground State T_e (cm^{-1}) of $^{138}Ba^{127}I$ in Different Methodologies

method[a]	$-E$	r_e	D_e[b]	ω_e	$\omega_e x_e$	a_e	$\bar{D}_e$	$\mu_{FF}(\langle\mu\rangle)$[c]	T_e
				X $^2\Sigma^+$					
MRCI	14801.80386	3.251	79.1 (73.2)	143	0.24	4.2	2.70	6.32 (6.27)	0.00
MRCI+Q	14801.8152	3.266	80.3 (74.4)	142	0.24	4.0	2.80	6.31	0.00
MRCI+DKH2	15240.27199	3.254	78.8 (71.1)	141	0.27	3.4	2.59	6.42 (6.34)	0.00
MRCI+DKH2+Q	15240.2781	3.257	75.1 (67.4)	141	0.23	3.0	2.33	6.45	0.00
C-MRCI	14801.96729	3.134	80.1 (74.2)	149	0.26	5.9	3.11	6.20 (5.62)	0.00
C-MRCI+Q	14802.0059	3.134	81.1 (75.2)	148	0.26	5.8	3.12	6.26	0.00
C-MRCI+DKH2	15240.44546	3.150	82.8 (75.1)					6.31 (5.92)	0.00
C-MRCI+DKH2+Q	15240.4675	3.140	76.0 (68.3)					6.21	0.00
RCCSD(T)	14801.81643	3.242	80.9 (74.4)	143	0.27	4.1	2.80	6.07	0.00
RCCSD(T)+DKH2	15240.28026	3.261	75.6 (67.9)	142	0.31	4.5	2.68	6.21	0.00
C-RCCSD(T)	14802.01144	3.137	80.7 (74.8)	147	0.22	6.4	3.25	6.21	0.00
C-RCCSD(T)+DKH2	15240.47018	3.136	77.0 (69.3)	146	0.30	6.4	3.36	6.35	0.00
expt[d]		3.0882	76.2 ± 1.5[e]	152.16	0.273	6.64	3.31	5.97[f]	0.00
				A′ $^2\Delta$					
MRCI	14801.77220	3.331	83.6	130	0.47	5.7	2.88	11.3 (11.6)	6955
MRCI+Q	14801.7824	3.341	84.0	130	0.45	5.8	2.86	11.3	7184
MRCI+DKH2	15240.22271	3.334	85.9	132	0.44	5.2	2.70	10.8(10.9)	10816
MRCI+DKH2+Q	15240.2296	3.346	81.0	132	0.48	5.5	2.26	10.5	10649
C-MRCI	14801.93641	3.224	83.1	132	0.34	6.4	3.49	10.8 (10.8)	6834
C-MRCI+Q	14801.9741	3.220	83.6	132	0.29	6.2	3.45	10.6	6974
C-MRCI+DKH2	15240.38845	3.203	83.9					10.6 (10.6)	12512
C-MRCI+DKH2+Q	15240.4161	3.192	79.4					10.4	11281
RCCSD(T)	14801.78341	3.338	84.1	129	0.33	5.8	5.06	11.3	7246
RCCSD(T)+DKH2	15240.22791	3.352	78.4	140	0.26	6.4	2.44	10.8	11491
C-RCCSD(T)	14801.97857	3.218	82.8	132	0.28	6.8	5.63	10.6	7214
C-RCCSD(T)+DKH2	15240.41870	3.188	80.8	135	0.29	6.8	3.93	10.4	11297
expt[g]		3.1216		142.29	0.274	6.93	5.09		8369.0
				A $^2\Pi$					
MRCI	14801.76710	3.333	56.0	129	0.58	5.6	2.93	8.83 (8.74)	8069
MRCI+Q	14801.7780	3.346	57.0	131	0.56	5.3	2.86	8.85	8148
MRCI+DKH2	15240.21751	3.307	44.6	135	0.59	6.9	3.19	7.56 (7.41)	11958
MRCI+DKH2+Q	15240.2238	3.316	41.0	133	0.68	7.6	3.21	7.62	11912
C-MRCI	14801.92910	3.243	56.0	130	0.27	8.0	3.36	8.92 (8.81)	8438
C-MRCI+Q	14801.9672	3.241	56.9	132	0.35	7.2	3.20	8.87	8476
C-MRCI+DKH2	15240.38933	3.202	47.6					7.53 (7.42)	12319
C-MRCI+DKH2+Q	15240.4131	3.195	41.8					7.58	11948
RCCSD(T)	14801.77883	3.339	56.7	128	0.35	6.0	3.01	9.25	8253
RCCSD(T)+DKH2	15240.22648	3.330	41.8	133	0.31	3.4	2.75	7.83	11803
C-RCCSD(T)	14801.97303	3.233	56.6	131	0.28	6.6	3.40	8.71	8430
C-RCCSD(T)+DKH2	15240.41571	3.190	42.8	135	0.26	6.9	3.46	7.62	11954
expt[h]		3.1388		141.75	0.275	7.02	3.46		9605.4
				B $^2\Sigma^+$					
MRCI	14801.76440	3.338	78.5	128	0.43	5.2	3.00	7.98 (7.86)	8661
MRCI+Q	14801.7750	3.347	79.6	129	0.47	5.0	2.90	7.88	8817
MRCI+DKH2	15240.22021	3.322	84.3	134	0.23	5.3	2.71	6.85 (6.72)	11364
MRCI+DKH2+Q	15240.2265	3.327	79.7	134	0.44	5.1	2.66	7.05	11324
C-MRCI	14801.92682	3.237	77.1	129	0.38	7.3	3.45	7.03 (7.75)	8938
C-MRCI+Q	14801.9646	3.232	77.6	129	0.34	7.1	3.53	6.78	9062
C-MRCI+DKH2	15240.38192	3.166	79.8					6.53 (6.41)	13944
C-MRCI+DKH2+Q	15240.4116	3.176	76.5					6.25	12280
RCCSD(T)	14801.77589	3.335	79.3	128	0.51	5.5	2.96	7.79	8897
RCCSD(T)+DKH2	15240.22570	3.312	77.1	132	0.38	4.5	2.83	7.16	11975
C-RCCSD(T)	14801.96885	3.235	76.7	130	0.59	6.8	3.46	6.76	9347
C-RCCSD(T)+DKH2	15240.41420	3.180	77.9	135	0.44	6.2	3.21	6.23	12286
expt[d]		3.1288		141.95	0.506	7.24	3.51		10427.0
				C $^2\Pi$					
MRCI	14801.71715	3.286	49.2	141	0.52	3.7	2.74	11.9 (12.1)	19032
MRCI+Q	14801.7293	3.288	50.9	143	0.57	3.0	2.70	11.8	18839
MRCI+DKH2	15240.17529	3.302	55.7	139	0.60	3.8	2.32	12.1 (12.6)	21363
MRCI+DKH2+Q	15240.1848	3.311	50.9	141	0.51	3.0	2.31	12.0	20474
C-MRCI	14801.88000	3.172	47.7	142	0.44	3.6	2.67	10.9 (11.1)	19214
C-MRCI+Q	14801.9210	3.154	50.3	149	0.39	6.0	3.06	10.5	18629
C-MRCI+DKH2	15240.33049	3.158	47.5					11.9 (11.8)	25232
C-MRCI+DKH2+Q	15240.3688	3.165	49.7					11.4	21674
RCCSD(T)	14801.73124	3.257	51.3	142	0.30	6.2	6.11	11.6	18696
RCCSD(T)+DKH2	15240.18680	3.276	52.6	144	0.34	5.9	2.61	12.3	20512
C-RCCSD(T)	14801.92319	3.164	48.0	147	0.21	6.7	2.36	10.5	19369
C-RCCSD(T)+DKH2	15240.37296	3.170	52.0	147				11.3	21337
expt[i]		3.0927		157.79	0.275	6.36	3.06		18188.5

TABLE 2 (Continued)

method[a]	$-E$	r_e	D_e[b]	ω_e	$\omega_e x_e$	a_e	$\bar{D}_e$	$\mu_{FF}(\langle\mu\rangle)$[c]	T_e
				D $^2\Sigma^+$					
MRCI	14801.69435	3.141	32.7	158	0.37	4.0	2.72	5.66 (6.02)	24796
MRCI+Q	14801.7060	3.153	35.8	157	0.49	4.3	2.70	5.64	24105
MRCI+DKH2	15240.15792	3.160	43.6	157	0.62	4.2	2.66	4.97 (6.04)	25138
MRCI+DKH2+Q	15240.1664	3.166	41.5	160				4.67	25049
C-MRCI	14801.86180	3.050	36.4	173	0.57	6.9	2.60	5.15 (5.77)	23152
C-MRCI+Q	14801.8962	3.031	34.7	176	0.35	7.3	2.59	5.24	24076
C-MRCI+DKH2	15240.31765	3.033	46.5					5.35 (6.01)	25569
C-MRCI+DKH2+Q	15240.3496	3.017	37.7					5.42	25876
expt[j]		3.0168		161.39	0.364	7.22	2.94		25775.1
				3 $^2\Pi$					
MRCI	14801.67307	4.400	21.4	104 ($=\Delta G_{1/2}$)					28706
MRCI+Q	14801.6855	4.352	23.2	91 ($=\Delta G_{1/2}$)					28465
				4 $^2\Sigma^+$					
MRCI	14801.65506	3.306	13.7						32658
MRCI+Q	14801.6705	3.296	17.4						31758
				5 $^2\Sigma^+$					
MRCI	14801.65032	3.670	10.7						33698
MRCI+Q	14801.6650	3.657	13.9						32965

[a] Internally contracted MRCI and C-MRCI calculations. +Q and DKH2 refer to the Davidson correction and to second-order Douglas−Kroll−Hess relativistic correction. [b] With respect to the adiabatic fragments of each state, i.e., $X^2\Sigma^+$ and $A^2\Pi$ to Ba(^{1}S) + I(^{2}P), whereas $A'^2\Delta$, $B^2\Sigma^+$, $C^2\Pi$, $D^2\Sigma^+$ to Ba(^{3}D) + I(^{2}P) and $4^2\Sigma^+$, $5^2\Sigma^+$ to Ba(^{1}D) + I(^{2}P). In the case of the $X^2\Sigma^+$ state binding energies in parentheses are reported with regard to Ba($^1S_0$) + I($^2P_{3/2}$). [c] $\langle\mu\rangle$ calculated as an expectation value, μ_{FF} through the finite field method. Electric field intensity 10^{-5} a.u. [d] References 26, 27, and 29. [e] Reference 25; dissociation energy with respect to Ba($^1S_0$) + I($^2P_{3/2}$). [f] Reference 21. [g] References 28 and 29. Note that the T_e value corresponds to the $A'^2\Delta_{3/2} \leftarrow X^2\Sigma^+$ electronic transition. [h] References 27 and 29. [i] References 18, 20, 26, 27, and 29. [j] Reference 29.

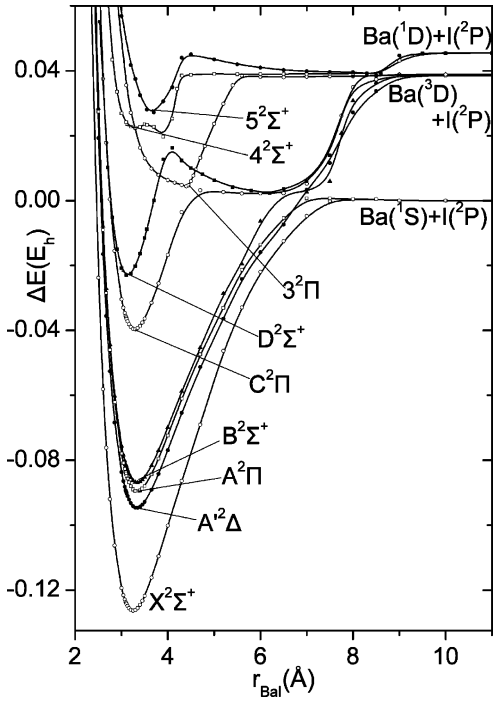

Figure 1. MRCI potential energy curves of the $^{2S+1}|\Lambda|$ states of BaI.

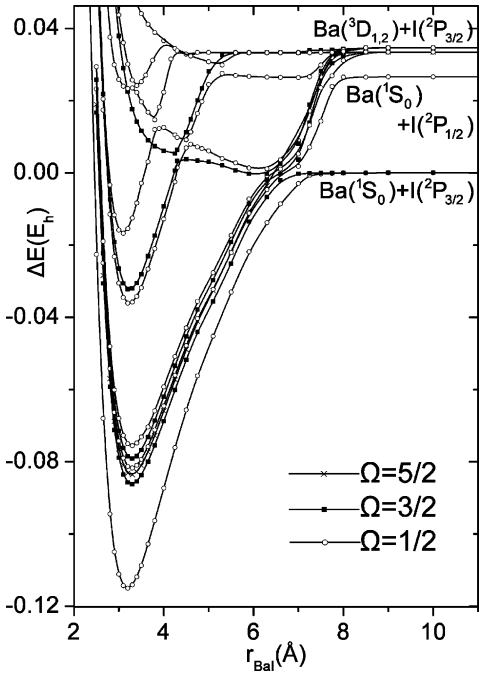

Figure 2. MRCI potential energy curves of the Ω states of BaI.

cm^{-1}.[29] Perhaps, it can be identified as either the $4^2\Sigma^+$ or $5^2\Sigma^+$ states listed in Table 2.

5. Spin−Orbit Coupling and Binding Energies

The experimental $^2P_{1/2} \leftarrow {}^2P_{3/2}$ SO splitting of I(^{2}P) atom is 7603.2 cm^{-1}, whereas those of the first excited state of Ba($^3D_{1\rightarrow2}$,$^3D_{1\rightarrow3}$) are smaller by more than an order of magnitude.[41] At the equilibrium however, the BaI molecule possesses a significant ionic character, and all states studied are related to $Ba^+(^2S_{1/2},{}^2D_{3/2,5/2},{}^2P_{1/2,3/2},{}^2S_{1/2}(7s^1)) + I^-(^1S_0)$ fragments. Because the SO splittings of the $^2D_{3/2,5/2}$ and $^2P_{1/2,3/2}$ atomic states of Ba^+ are 801.0 and 1690.8 cm^{-1}, respectively, and that of $I^-(^1S_0)$ is zero, one expects that the SO splittings of the molecular states ($\Lambda \neq 0$) to be around 1000 cm^{-1}. Indeed, for the $A'^2\Delta_{5/2\leftarrow3/2}$, $A^2\Pi_{3/2\leftarrow1/2}$, and $C^2\Pi_{3/2\rightarrow1/2}$ states, the C-MRCI (C-MRCI+DKH2) SO splittings are 665 (615), 494 (578), and 811 (1002) cm^{-1}, respectively, as contrasted to the experimental values 656.66 ($A^2\Pi_{3/2\leftarrow1/2}$) and 756.06 ($C^2\Pi_{3/2\leftarrow1/2}$) cm^{-1}.[27] No experimental SO values exist for the $A'^2\Delta_{5/2\leftarrow3/2}$ transition.

Within the $\Omega(\omega,\omega)$ coupling [Λ, Σ are not defined, Hund's case (c)], the lower asymptotic neutral atoms Ba($^1S_0$) + I($^2P_{3/2}$) give rise to $\Omega = {}^1/_2$ and $^3/_2$. As we move up the energy ladder, we obtain Ba($^1S_0$) + I($^2P_{1/2}$) → $\Omega = {}^1/_2$; Ba($^3D_1$) + I($^2P_{3/2}$) → $\Omega = {}^1/_2$ [3], $^3/_2$ [2], $^5/_2$ [1] (numbers in square brackets indicate

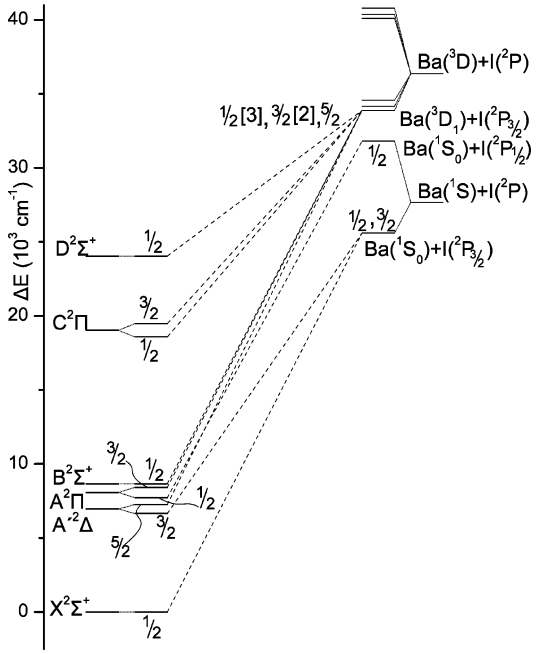

Figure 3. Correlation $^{2S+1}|\Lambda| - \Omega(\omega,\omega)$ diagram of BaI.

the number of Ω states); and Ba(^{3}D$_2$) + I(^{2}P$_{3/2}$) → Ω = $^1/_2$ [4], $^3/_2$ [3], $^5/_2$ [2], $^7/_2$ [1], etc. Figure 2 displays PECs assigned according to their Ω good quantum numbers; Figure 3 shows a diagram of the Λ−Σ states (on the left) and their Ω splittings (middle) correlating to the corresponding asymptotic Ω atomic states (on the right).

From Figure 3 we see that the X-state (Ω = $^1/_2$) correlates uniquely to the $^1/_2$ Ω-component of Ba(^{1}S$_0$) + I(^{2}P$_{3/2}$). In discussing the dissociation of the ground state of BaI, the I(^{2}P$_{1/2}$←^{2}P$_{3/2}$) splitting has been taken into account (vide supra), resulting finally to 66.2 kcal/mol, about 10 kcal/mol smaller than the experimental one. We examine now the binding energies of the A′^{2}Δ, A^{2}Π, and B^{2}Σ$^+$ states. It is clear from Figure 3 that the A′^{2}Δ(Ω=$^3/_2$) correlates to the Ω = $^3/_2$ of Ba(^{1}S$_0$) + I(^{2}P$_{3/2}$) (see also Figure 2); however, in the Λ−Σ scheme the A′^{2}Δ state correlates to Ba(^{3}D) + I(^{2}P). With respect to those end products D_e = 77.5 kcal/mol, the average of the C-MRCI+DKH2+Q and C-RCCSD(T)+DKH2 D_e values (80.1 kcal/mol, see Table 2), corrected for the average BSSE of the X^{2}Σ$^+$ state. This value should be reduced by the calculated at the same level gap ΔE(^{3}D−^{1}S) of Ba (∼12600 cm^{-1}, Table 1) and the $^1/_3$ of the I (^{2}P$_{1/2}$−^{2}P$_{3/2}$) SO splitting (8052 cm^{-1}), and increased by $^1/_2$ of A′^{2}Δ($^5/_2$−$^3/_2$) splitting (∼635 cm^{-1}). Therefore, D_e(A′^{2}Δ; Ω=$^3/_2$) = 77.5 kal/mol − 12600 cm^{-1} − 8052/3 cm^{-1} + 635/2 cm^{-1} = 34.7 kcal/mol. Alternatively, because the X^{2}Σ$^+$(Ω=$^1/_2$) and A′^{2}Δ(Ω=$^3/_2$) correlate to the same end products ($^1/_2$, $^3/_2$), the D_e value can be calculated directly by subtracting the X^{2}Σ$^+$−A′^{2}Δ energy separation (11290 cm^{-1}) from the binding energy (66.2 kcal/mol) of the X-state and adding half of the A′^{2}Δ($^5/_2$−$^3/_2$) splitting: D_e(A′^{2}Δ; Ω=$^3/_2$) = 66.2 kcal/mol − 11290 cm^{-1} + 635/2 cm^{-1} = 34.8 kcal/mol. The experimental dissociation energy of the A′^{2}Δ(Ω=$^3/_2$) state is obtained directly by using the experimental X$^2\Sigma^+_{1/2}$ − A′$^2\Delta_{3/2}$ separation energy T_e = 8369.0 cm^{-1},[28,29] i.e., $D_e^{Expt} = D_e^{Expt}$(X$^2\Sigma^+_{1/2}$) − T_e^{Expt} = 76.2 ± 1.5 kcal/mol[25] − 8369.0 cm^{-1} = 52.3 ± 1.5 kcal/mol. The 17 kcal/mol difference from the theoretical value can be clearly traced to the 10 kcal/mol difference in the X^{2}Σ$^+$ calculated D_e, and the calculated Ba(^{3}D−^{1}S) difference, in error by about 8 kcal/mol with respect to experiment (Table 1).

TABLE 3: Λ−Σ, Ω(ω,ω), and Experimental Dissociation Energies D_e (kcal/mol) of the First Six Λ−Σ or Nine Ω States of BaI

state (Λ−Σ)	D_e(Λ−Σ)[a]	state (Ω)	D_e(Ω)	D_e(expt)[b]
X^{2}Σ$^+$	73.9	1/2	66.2	76.2 ± 1.5[c]
A′^{2}Δ	77.5	3/2	34.8	52.3 ± 1.5
		5/2	68.1	76.3 ± 1.5
A^{2}Π	39.7	1/2	55.9	71.4 ± 1.5
		3/2	66.3	73.6 ± 1.5
B^{2}Σ$^+$	74.6	1/2	66.2	72.2 ± 1.5
C^{2}Π	48.2	1/2	41.2	51.1 ± 1.5
		3/2	38.3	48.9 ± 1.5
D^{2}Σ$^+$	35.1	1/2	27.3	28.3 ± 1.5

[a] The Λ−Σ D_e values have been obtained from Table 2 through the formula D_e(Λ−Σ) = 1/2[D_e(C-MRCI+DKH2+Q) + D_e(C-RCCSD(T)+DKH2)] − BSSE(X^{2}Σ$^+$). In the case of the D^{2}Σ$^+$ state D_e(Λ−Σ) = D_e(C-MRCI+DKH2+Q) − BSSE(X^{2}Σ$^+$). [b] The D_e(expt) values based on the Ω(ω,ω) coupling were obtained indirectly from the experimental value of the X$^2\Sigma^+_{1/2}$ state; see text. [c] Reference 25.

Now, the Ω = $^5/_2$ component of the A′^{2}Δ state correlates uniquely to Ω = $^5/_2$ stemming from the Ba(^{3}D$_1$) + I(^{2}P$_{3/2}$) end products (Figure 3).We estimate the experimental D_e(Ω=$^5/_2$) from the relation (see Figure 3), D_e^{Expt}(A′^{2}Δ; Ω=$^5/_2$) = D_e^{Expt}(X$^2\Sigma^+_{1/2}$) − T_e^{Expt}(X$^2\Sigma^+_{1/2}$−A′$^2\Delta_{3/2}$) − ΔE(A′$^2\Delta_{3/2-5/2}$) + T_e^{Expt}(Ba;^{3}D$_1$−^{1}S$_0$). The A′$^2\Delta_{3/2-5/2}$ experimental splitting is unknown; instead we use the calculated one, therefore D_e^{Expt}(A′^{2}Δ;Ω=$^5/_2$) = 76.2 ± 1.5 kcal/mol − 8369.0 cm^{-1} − 635 cm^{-1} + 9034 cm^{-1} (ref 41) = 76.3 ± 1.5 kcal/mol. It is interesting that the (experimental) dissociation energy of the two Ω components of the A′^{2}Δ state, $^3/_2$ and $^5/_2$, differ by 24 kcal/mol. The theoretical value of the Ω = $^5/_2$(A′^{2}Δ) can be obtained by using the corresponding calculated quantities, i.e., D_e(A′^{2}Δ;Ω=$^5/_2$) = D_e(X$^2\Sigma^+_{1/2}$) − T_e(A′^{2}Δ−X^{2}Σ$^+$) − ΔE(A′$^2\Delta_{3/2-5/2}$)/2 + T_e(Ba;^{3}D$_1$−^{1}S$_0$), where T_e(Ba;^{3}D$_1$−^{1}S$_0$) = ΔE(Ba;^{3}D−^{1}S) − ΔE(Ba;^{3}D−^{3}D$_1$) = 12600 cm^{-1} − 326 cm^{-1} (C-MRCI+DKH2) = 12274 cm^{-1}. Therefore, D_e(A′^{2}Δ; Ω=$^5/_2$) = 66.2 kcal/mol − 11290 cm^{-1} − $^1/_2$ × 635 cm^{-1} + 12274 cm^{-1} = 68.1 kcal/mol. This calculated D_e value compares favorably with the experimental one previously obtained due to the cancellation of the T_e(A′^{2}Δ−X^{2}Σ$^+$) and T_e(Ba;^{3}D$_1$−^{1}S$_0$) separations. The remaining error is traced again to the underestimation by 10 kcal/mol of the D_e value of the X$^2\Sigma^+_{1/2}$ state.

Following the same line, we obtain the experimental binding energies of Ω = $^1/_2$ and $^3/_2$ of the A^{2}Π state, the Ω = $^1/_2$ of B^{2}Σ$^+$, the Ω = $^1/_2$ and $^3/_2$ of C^{2}Π, and the Ω = $^1/_2$ of D^{2}Σ$^+$, along with the corresponding D(Ω) theoretical values. Note that the A^{2}Π(Ω=$^1/_2$) correlates to Ba(^{1}S$_0$) + I(^{2}P$_{1/2}$), whereas the rest of the states correlate to Ba(^{3}D$_1$) + I(^{2}P$_{3/2}$). All our results on the dissociation energies (including the X$^2\Sigma^+_{1/2}$ and A′$^2\Delta_{3/2,5/2}$ states) are listed in Table 3. It is obvious from the results shown in Table 3 that the Ω-approach is mandatory for obtaining sensible binding energies in the present case. The "experimental" D_e values listed in Table 3 are all based on the dissociation energy of the X$^2\Sigma^+_{1/2}$ state, and as far as we know, they are estimated for the first time. With the exception of the D^{2}Σ$^+$(Ω=$^1/_2$) state, where the agreement of the dissociation energy between theory and experiment is perfect, the D_e values of the rest of the states differ on the average by 10 kcal/mol, the calculated ones being smaller. As was mentioned previously, this discrepancy can be traced mainly to the underestimated D_e value of the X$^2\Sigma^+_{1/2}$ state.

6. Summary and Remarks

For the first time *ab initio* calculations are reported for the heavy molecule BaI, using variational multireference and single reference coupled cluster methods in conjunction with medium size basis sets. The role of relativity was also considered through the DKH2 approximation. For the six $\Lambda-\Sigma$ states, namely $X^2\Sigma^+$, $A'^2\Delta$, $A^2\Pi$, $B^2\Sigma^+$, $C^2\Pi$, and $D^2\Sigma^+$, we have calculated full potential energy curves, dissociation energies, common spectroscopic parameters, and dipole moments. For three more states lying about 30000 cm^{-1} above the ground state, that is $3^2\Pi$, $4^2\Sigma^+$, and $5^2\Sigma^+$, our calculations are only indicative and very limited. Besides the obvious difficulties for such a system, heavy nuclei and low-quality basis sets, the calculations and interpretations are also plagued by multiple avoided crossings from ionic states. Therefore, the present work can be considered as a first effort to better understand BaI, and perhaps to provide some useful information within the corpus of "conventional" quantum mechanical methods. Our main conclusions can be epitomized as follows.

In all states studied the equilibrium structures are quite ionic with a Mulliken charge transfer from Ba to I of about 0.5 electron. Dipole moments are expected to be quite large and indeed they are, ranging from around 6 ($X^2\Sigma^+$) to 11 ($C^2\Pi$) D. Because the agreement between the calculated dipole moment of the $X^2\Sigma^+$ state and the experimental one is good, 6.2 vs 5.97 (expt) D, we believe that the calculated dipole moments for the rest of the states should be reliable enough.

Dissociation energies proved more problematic because of strong spin−orbit couplings. To obtain sensible results the Ω-(ω,ω) scheme coupling was deemed as necessary to correlate the equilibrium structures with the correct end products. For the ground state ($X^2\Sigma^+$; $\Omega=1/2$) a binding energy of 66.2 kcal/mol is obtained, 10 kcal/mol less than the experimental number. After identifying our end Ω-products we were able for the first time to derive experimental D_e values by employing the experimental $D_e(\Omega)$ value of the $X^2\Sigma^+_{1/2}$ state. Our calculated $D_e(\Omega)$ values for the first nine Ω-states are on the average underestimated by 10 kcal/mol with respect to the estimated experimental values.

Our general conclusion is that useful information can be extracted by using more or less conventional calculation methods even for systems as heavy as the BaI molecule.

Acknowledgment. We thank the referee for his (her) insightful comments. E.M. expresses his gratitude to Hellenic Scholarships Foundation (I.K.Y.) for financial support.

References and Notes

(1) De Boisbaudran, M. L. *Compt. Rend.* **1870**, *70*, 974.
(2) Olmsted, C. M. *Z. Wiss. Photographie* **1906**, *4*, 255.
(3) Walters, O. H.; Barratt, S. *Proc. R. Soc. London A* **1928**, *118*, 120.
(4) Mesnage, P. *Ann. Phys.* **1939**, *12*, 5.
(5) Patel, M. M.; Shah, N. R. *Ind. J. Pure Appl. Phys.* **1970**, *8*, 681.
(6) Dagdigian, P. J.; Cruse, H. W.; Zare, R. N. *J. Chem. Phys.*, **1974**, *60*, 2330.
(7) Bradford, R. S., Jr.; Jones, C. R.; Southall, L. A.; Broida, H. P. *J. Chem. Phys.* **1975**, *62*, 2060.
(8) Dickson, C. R.; Kinney, J. B.; Zare, R. N. *Chem. Phys.* **1976**, *15*, 243.
(9) Shah, S. G.; Patel, M. M. *Indian J. Pure Appl. Phys.* **1977**, *15*, 728.
(10) Rao, M. L. P.; Rao, D. V. K.; Rao, P. T.; Murty, P. S. *Fizika* **1977**, *9*, 25.
(11) Estler, R. C.; Zare, R. N. *Chem. Phys.* **1978**, *28*, 253.
(12) Kleinschmidt, P. D.; Hildenbrand, D. L. *J. Chem. Phys.* **1978**, *68*, 2819.
(13) Johnson, M. A.; Webster, C. R.; Zare, R. N. *J. Chem. Phys.* **1981**, *75*, 5575.
(14) Johnson, M. A.; Noda, C.; Mc Killop, J. S.; Zare, R. N. *Can. J. Phys.* **1984**, *62*, 1467.
(15) Törring, T.; Döbl, K. *Chem. Phys. Lett.* **1985**, *115*, 328.
(16) Johnson, M. A.; Zare, R. N. *J. Chem. Phys.* **1985**, *82*, 4449.
(17) Ernst, W. E.; Kändler, J.; Noda, C.; Mc Killop, J. S.; Zare, R. N. *J. Chem. Phys.* **1986**, *85*, 3735.
(18) Zhao, D.; Vaccaro, P. H.; Tsekouras, A. A.; Leach, C. A.; Zare, R. N. *J. Mol. Spectrosc.* **1991**, *148*, 226.
(19) Leach, C. A.; Waldeck, J. R.; Noda, C.; Mc Killop, J. S.; Zare, R. N. *J. Mol. Spectrosc.* **1991**, *146*, 465.
(20) Leach, C. A.; Tsekouras, A. A.; Zare, R. N. *J. Mol. Spectrosc.* **1992**, *153*, 59.
(21) Ernst, W. E.; Kändler, J.; Törring, T. *Chem. Phys. Lett.* **1986**, *123*, 243.
(22) Fernando, W. M. L.; Douay, M.; Bernath, P. F. *J. Mol. Spectrosc.* **1990**, *144*, 344.
(23) Douay, M.; Brazier, C.; Bernath, P. F. Unpublished results as quoted in ref 22.
(24) Vaccaro, P. H.; Zhao, D.; Tsekouras, A. A.; Leach, C. A.; Ernst, W. E.; Zare, R. N. *J. Chem. Phys.* **1990**, *93*, 8544.
(25) Hildenbrand, D. L.; Lau, K. H. *J. Chem. Phys.* **1992**, *96*, 3830.
(26) Gutterres, R. F.; Vergès, J.; Amiot, C. *J. Mol. Spectrosc.* **1999**, *196*, 29.
(27) Gutterres, R. F.; Vergès, J.; Amiot, C. *J. Mol. Spectrosc.* **2000**, *200*, 253.
(28) Gutterres, R. F.; Vergès, J.; Amiot, C. *J. Mol. Spectrosc.* **2000**, *201*, 326.
(29) Gutterres, R. F.; Fellows, C. E.; Vergès, J.; Amiot, C. *J. Mol. Spectrosc.* **2001**, *206*, 62.
(30) Törring, T.; Ernst, W. E.; Kändler, J. *J. Chem. Phys.* **1989**, *90*, 4927.
(31) Törring, T.; Ernst, W. E.; Kindt, S. *J. Chem. Phys.* **1984**, *81*, 4614.
(32) Rice, S. F.; Martin, H.; Field, R. W. *J. Chem. Phys.* **1985**, *82*, 5023.
(33) Arif, M.; Jungen, C.; Roche, A. L. *J. Chem. Phys.* **1997**, *106*, 4102.
(34) Raouafi, S.; Jungen, C. *Phys. Essays* **2000**, *13*, 272.
(35) Huzinaga, S.; Miguel, B. *Chem. Phys. Lett.* **1990**, *175*, 289. Huzinaga, S.; Klobukowski, M. *Chem. Phys. Lett.* **1993**, *212*, 260.
(36) Raghavachari, K.; Trucks, G. W.; Pople, J. A.; Head-Gordon, M. *Chem. Phys. Lett.* **1989**, *157*, 479. Bartlett, R. J.; Watts, J. D.; Kucharski, S. A.; Noga, J. *Chem. Phys. Lett.* **1990**, *165*, 513; **1990**, *167*, 609E. Knowles, P. J.; Hampel, C.; Werner, H.-J. *J. Chem. Phys.* **1993**, *99*, 5219; **2000**, *112*, 3106E.
(37) Werner, H.-J.; Knowles, P. J. *J. Chem. Phys.* **1988**, *89*, 5803. Knowles, P. J.; Werner, H.-J. *Chem. Phys. Lett.* **1988**, *145*, 514. Werner, H.-J.; Reinsch, E. A. *J. Chem. Phys.* **1982**, *76*, 3144. Werner, H.-J. *Adv. Chem. Phys.* **1987**, *LXIX*, 1.
(38) MOLPRO, version 2002.6, is a package of ab initio programs designed by H.-J. Werner, P. J. Knowles, R. D. Amos, et al.; see http://www.molpro.net.
(39) Douglas, M.; Kroll, N. M. *Ann. Phys.* **1974**, *82*, 89. Hess, B. A. *Phys. Rev. A* **1985**, *32*, 756; **1986**, *33*, 3742. Jansen, G.; Hess, B. A. *Phys. Rev. A* **1989**, *39*, 6016.
(40) Boys, S. F.; Bernardi, F. *Mol. Phys.* **1970**, *19*, 553. Liu, B.; McLean, A. D. *J. Chem. Phys.* **1973**, *59*, 4557. Jansen, H. B.; Ros, P. *Chem. Phys. Lett.* **1969**, *3*, 140.
(41) Moore, C. A. Atomic Energy Levels; NRSDS-NBS, Circ. No. 35; U.S. GPO: Washington, DC, 1971.
(42) Hanstorp, D.; Gustafsson, M. *J. Phys. B: At. Mol. Opt. Phys.* **1992**, *25*, 1773.